Journal of Advanced Informatics in Water, Soil, and Structure

journal homepage: www.wss.torbath.ac.ir

Research Article

Numerical Analysis of The Interlayer Behaviour of a Steel-Concrete-Steel Sandwich Structure with Corrugated-Strip Shear Connectors

Mohammad Golmohammadi[a], *Mehdi Yousefi*[b]

[a] *Civil Engineering Department, Faculty of Engineering, University of Torbat Heydarieh, Torbat Heydarieh, Iran*

[b] *Civil Engineering Department, Faculty of Maritime Engineering, Chabahar Maritime University, Chabahar, Iran*

ARTICLE INFO

Received date: 22 Apr 2025
Accept date: 27 Oct 2025
Published date: 01 Nov 2025

Keywords:
Steel-Concrete-Steel Sandwich; Corrugated-Strip Connectors; Finite Element Model; Shear Strength

Abstract

Steel-concrete-steel (SCS) sandwich composite structures consist of two steel face plates and a concrete core connected by shear connectors. Due to their high strength-to-weight ratio and excellent energy dissipation capacity, these systems are increasingly used in offshore structures. This study develops 211 numerical models using the Explicit solver and mass-scaling technique in ABAQUS to efficiently simulate quasi-static behavior despite geometric complexities. The models investigate the influence of key geometric parameters—including steel face plate thickness, concrete core thickness, and concrete compressive strength—on the shear performance of corrugated strip connectors (CSC). A major contribution of this research is the formulation of predictive linear regression equations for estimating maximum shear strength, offering a practical and time-efficient tool for the preliminary design and optimization of SCS structures. The findings demonstrated the critical influence of connector geometry and concrete strength on the shear performance of SCS sandwich structures, and improved predictive accuracy was achieved through refined numerical modeling.

Homepage: www.wss.torbath.ac.ir

*Corresponding Author:
Golmohammadi Mohammad
Email: m.golmohammadi@torbath.ac.ir
ORCID: 0000-0001-8620-4159

https://doi.org/10.22048/WSS.2025.518550.1018

How to cite this article:

Golmohammadi, M. & Yousefi, M. (2025). Numerical Analysis of the Interlayer Behaviour of a Steel-Concrete-Steel Sandwich Structure with Corrugated-Strip Shear Connectors. *Journal of Advanced Informatics in Water, Soil, and Structure*, *2*(2), 219-234.

Introduction

One of the modern products formed by changing the geometrical combination of common materials in building works, i.e. steel and concrete, is steel-concrete-steel (SCS) sandwich structures. A SCS sandwich structure is composed of two steel face plates with a concrete core that are connected using adhesive materials or mechanical shear connectors. Experimental researches have shown that mechanical shear connectors have advantages over adhesive materials in terms of transverse shear strength (Solomon et al., 1976). The use of SCS structures is being noticed in the building and offshore structures industries due to their cost effectiveness, high strength-to-weight ratio, and high energy dissipation, especially against impact and explosion. The type of concrete and shear connectors are research issues that different researchers have examined to improve the performance of this system.

Recent studies have focused on enhancing the structural behavior of SCS systems through innovative connector configurations and advanced modelling techniques. Khatibi et al. (2022, 2023) and Daliri et al. (2025; 2025) investigated box-profile shear connectors and proposed validated numerical models to assess flexural and shear performance. Yousefi, Golmohammadi, and Khatibi (2023) developed predictive models using gene expression programming (GEP) to estimate punching shear strength in SCS slabs with stud-bolt connectors. These approaches offer improved accuracy and efficiency in simulating complex connector geometries. Ghalehnovi and Yousefi have also contributed to the development of DSCS systems with corrugated-strip connectors, emphasizing the role of connector orientation and welding configuration in enhancing interlayer shear resistance.

In Fig. 1, a SCS system is shown with the most common shear connectors analysed by researchers. In Fig. 1(a), stud shear connectors in double skin system (DSC), whose main advantage is their easy application, are shown (Tomlinson et al., 1990). The drawbacks of this system are the fact of requiring a uniform thickness, the local buckling of the steel face plates and unsuitable behaviour against cyclic loading due to the connection of one end to steel face plates (Dogan & Roberts, 2012). Although, according to Fig. 1(b), using bi-steel shear connectors removed these problems, the minimum thickness of 20 cm and the need for modern equipment for friction welding have limited using bi-steel systems (Bowerman & Chapman, 2000). Hence, according to Fig. 1(c), shear connectors with interlocked hooks or J-hook shear connectors are proposed (Liew, 2008; Liew & Sohel, 2009). Although the structural behaviour of SCS systems with J-hook shear connectors may not be as good as that of bi-steel system because the length of the hooks may increase, it did not have any of the limitations of the previous shear connectors. Hence, extensive researches have been performed on the structural behaviour of the system (Yan et al., 2015a; Yan, Liew, Sohel, et al., 2014; Yan et al., 2015b; Yan, Liew, Zhang, et al., 2014). One limitation of using these shear connectors is the need for a special jaw to use the stud shear-welding device. One of the SCS systems that has received limited attention in the literature is the configuration with corrugated strip shear connectors (CSC), as shown in Fig. 1(d). The advantage of this system is to set the branches of the shear connectors perpendicular to the crack development path (Leekitwattana et al., 2011). The important reason of non-development of the system is application problems that are created by welding the two ends to the steel face plates.

To apply CSCs as in Fig. 2, a double-skin system with corrugated-strip connectors (DSCS) was proposed with some changes, in which CSC shear connectors are applied as one end welded like in the DSC system (Yousefi & Ghalehnovi, 2017). To examine the interlayer shear behaviour, push-out tests were performed on some test specimens and relations were proposed to predict the load-slip behaviour and interlayer maximum shear strength. Although the interlayer shear strength of the system is about half of that of the bi-steel strength, due to being one end welded, its advantages include setting CSCs branches along the crack development path, easy application and accessibility of materials. The parameters that affect the interlayer shear behaviour of DSCS systems are the characteristics of the materials and their geometry. Given the high number of geometrical parameters that affect the behaviour of the system, the effect of some of them was examined in the experiments performed without changing the mechanical characteristics of the core materials. Due to the complicated behaviour of DSCS system because of the high number of

geometrical parameters, the experimental examinations require many push-out tests. Therefore, in this study, the interlayer shear behaviour of DSCS system is developed using the numerical analysis.

(a) Stud shear connectors in DSC system

(b) Two end welded connectors in Bi-steel system

(c) J-hook shear connectors

(d) Corrugated strip shear connectors (CSC)

Figure 1. Shear connectors in SCS sandwich structures

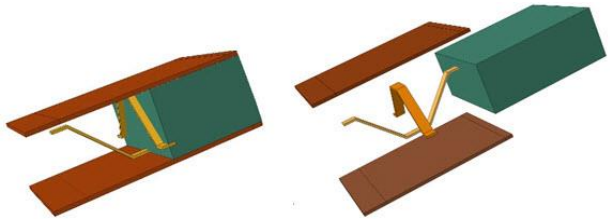

Figure 2. The proposed SCS sandwich structure (Yousefi & Ghalehnovi, 2017)

Among the analytical approaches, numerical methods—particularly finite element (FE) analysis—have proven to be powerful tools for investigating the structural behavior of steel-concrete-steel (SCS) sandwich systems. Although early studies offered limited insight into the finite element analysis (FEA) of corrugated strip shear connectors (CSC), recent research has significantly advanced the modeling of various SCS configurations.

For example, Yousefi et al. (2023; 2018; 2021) developed validated FE models for double-skin SCS systems with CSC connectors, incorporating mass-scaling techniques in Explicit solvers to achieve efficient quasi-static simulations. Khatibi et al. (2023) investigated box-profile shear connectors and conducted comprehensive numerical and experimental studies to evaluate their flexural and shear performance. Yousefi, et al. (2023) applied gene expression programming (GEP) to predict punching shear strength in SCS slabs with stud-bolt connectors, demonstrating the potential of AI-assisted modelling in structural analysis. Huang et al. (2013), as well as Yan et al. (2016), have contributed extensively to the numerical simulation of SCS systems with J-hook and bi-steel connectors, addressing complex geometries and connector interactions through advanced FE techniques.

More recently, Barahouei et al. (2025) conducted experimental and numerical investigations on the flexural behavior of SCS beams with two-end welded C-shape shear connectors and reactive powder concrete (RPC) cores. Their study introduced a refined FE model that accurately captured the interaction between connectors and RPC, offering improved predictions of load-deflection response and failure mechanisms. In a complementary study, the same authors proposed a parametric numerical framework to evaluate the influence of connector geometry and concrete type on the overall performance of SCS beams under bending loads.

Earlier simplified models, such as those developed for double-skin structures with overlapping stud shear connectors (Shanmugam et al., 2002), treated the concrete core as a homogeneous anisotropic material and neglected explicit connector modelling. While these approaches improved computational efficiency, they failed to capture the true interaction between shear connectors and concrete, potentially underestimating transverse shear strength. Similar simplifications were adopted by Zou and Xia et al. (2016), who analyzed failure mechanisms in SCS beams without modelling connectors, relying solely on steel-concrete interface behavior.

Other modeling strategies include the use of nonlinear spring elements to represent stud shear connectors (Smitha & Kumar, 2013), and two-

dimensional FE models for bi-steel beams (Foundoukos & Chapman, 2008), which limit the simulation of inherently three-dimensional connector-concrete interactions. In SCS systems with J-hook connectors, the interlocking mechanism plays a critical role in transferring longitudinal shear, resisting transverse forces, and preventing local buckling of steel plates. However, the complex geometry of these connectors poses challenges for FE modeling. To address this, some studies have replaced the hook geometry with nonlinear spring elements to simulate connector interaction (Huang & Liew, 2016; Yan, 2015). More recent works have developed full three-dimensional FE models that accurately capture the shear-interfacial slip and axial tension behavior of J-hook connectors, validated against push-out and pull-out tests .

One method that increases the analysis speed despite geometrical complexities and maintains the required accuracy is the mass-scaling technique in Explicit analysis to simulate quasi-static (ABAQUS, 2010). In previous studies, Yousefi and Ghalehnovi (2018) investigated the finite element modeling (FEM) of DSCS systems with complex geometries and proposed numerical models using the Explicit solver and mass-scaling method in ABAQUS, which were validated through push-out tests (Yousefi & Ghalehnovi, 2017).

However, despite these efforts, a comprehensive parametric investigation into the influence of key geometrical parameters of corrugated strip shear connectors (CSC) in DSCS systems remains absent from the literature. In this study, a total of 211 numerical models are developed to systematically examine the effects of CSC geometry, steel face plate thickness, concrete core thickness, and concrete compressive strength on the interlayer shear behavior. The results are evaluated in terms of failure modes, load-slip behavior, and maximum shear strength. As a novel contribution, this research introduces predictive regression equations derived from the numerical results to estimate the maximum shear strength of DSCS systems with CSC connectors. These equations are then compared with empirical relations extracted from experimental data to assess their accuracy and applicability. This approach addresses a critical gap in existing studies by offering a validated and efficient framework for predicting shear performance in DSCS structures with complex connector geometries.

FE model for push-out test

According to Fig. 3, the elements of the push-out test, including steel face plates, shear connectors, concrete core and load cell, are modelled using a three dimensional 10-node modified quadratic tetrahedron continuous element (C3D10M). For a pair of DSCS shear connectors, the specimen is prepared in FE model by taking into account the structural symmetry and loading. Mesh sizes of 9, 10, 12, 15, and 20 mm were evaluated, and ultimately, a uniform mesh size of 9 mm was selected for all sections of the model. According to Fig. 3, in the bond between the shear connectors and steel face plates and the positions of the contact between the shear connectors and the concrete core, a finer mesh size is used for a better simulation. The method of modelling the concrete and steel materials and the boundary conditions, loading and solution methods are described in detail in the work by Yousefi and Ghalehnovi (2018). The concrete materials used in the tests have the compressive strength 37 MPa and the mechanical characteristics of the steel used are as in Table 1.

So that the numerical models have a quasi-static behaviour, the kinetic energy was controlled not to exceed 5% to 10% of the internal energy in all models as in Fig. 4. In addition, as in the diagram of specimen 6D-1, the kinetic energy did not have many oscillations in the other specimens.

According to Fig. 5, in addition to confirming the validity of the finite elements models, push-out test on 12 DSCS specimens shows that the structures can be analysed with complicated interactions with an acceptable speed and accuracy.

Numerical analysis of the shear connectors in the DSCS

According to 12 valid numerical models addressed in the previous section, changing the mechanical properties of the concrete including f_c and E_c and the geometrical parameters on the validated models, 211 finite elements models are developed in this section. Geometrical parameters include: thickness of the steel face plates, t_p; ratio of the width of the shear connector to its thickness,

$b_t = b_c / t_c$; angle of the shear connectors branches compared to the steel face plates in radian, θ_r; ratio of the height of the shear connectors to the concrete thickness, $\boldsymbol{h_h = h_c/h_{con}}$; overlapping length of the right and left shear connectors, I_c; and ratio of the width of the shear connector to concrete width, $k_{cb} = b_c / b$.

Next, the effect of each parameter on the failure modes and load-slip behaviour is evaluated and relations are proposed to estimate the ultimate shear strength.

3-1 Naming the numerical models

The numerical models are designated using the format t_pX_1-f_cX_2-aX_3-hX_4-$h_{con}X_5$-b_cX_6-t_cX_7, where each prefix corresponds to a specific geometric or material parameter:

- t_p: thickness of the steel face plates (mm)
- f_c: compressive strength of the concrete core (MPa)
- a: inclination angle of the shear connector branches (degrees)
- h: height of the shear connector branches (mm)

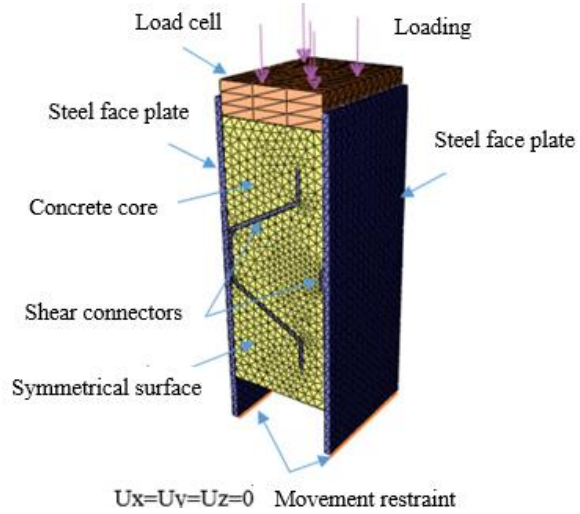

Figure 3. Finite elements model for push-out test (Yousefi & Ghalehnovi, 2018)

Table 1. Mechanical characteristics of steel extracted from the direct tension test (Yousefi & Ghalehnovi, 2017)

Thickness (mm)	0.2% proof stress (MPa)	Ultimate stress (MPa)	ε_s in ultimate stress	E_s (GPa)
4	250	380	0.3	207
6	285	495	0.23	202
8	411	615	0.176	205
10	367	620	0.198	203
12	310	516	0.180	207

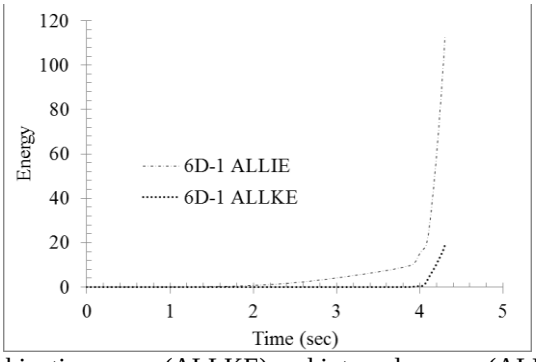

Figure 4. Comparison of the kinetic energy (ALLKE) and internal energy (ALLIE) of the numerical model of the specimen 6D-1 (Yousefi & Ghalehnovi, 2018)

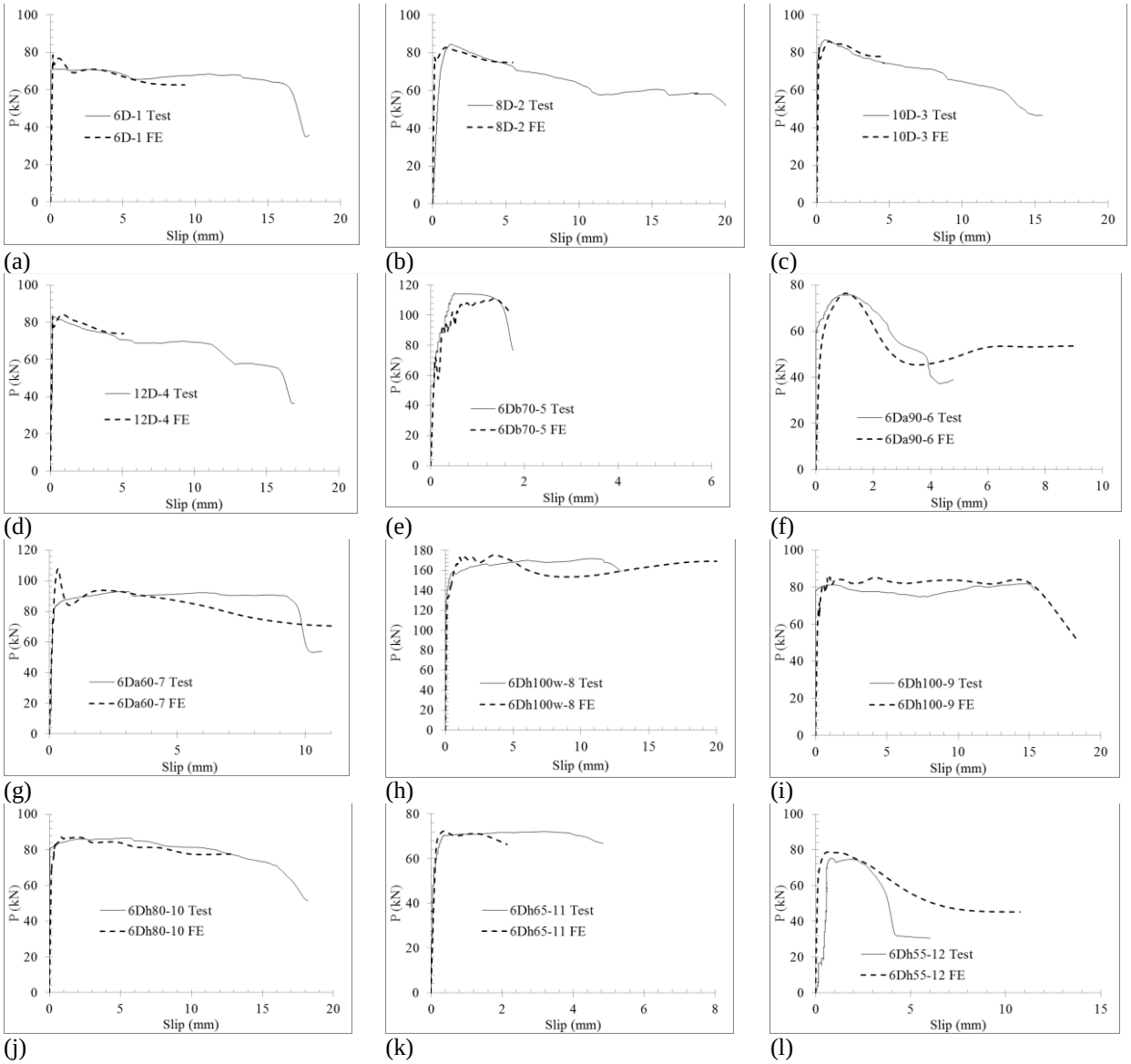

Figure 5. Comparison of the load-slip curve between tests and finite element models (Yousefi & Ghalehnovi, 2018)

- h_{con}: thickness of the concrete core (mm)
- b_c: width of the shear connectors (mm)
- t_c: thickness of the shear connectors (mm)

The variables X_1 through X_7 represent the numerical values assigned to each parameter. In cases where any of the parameters t_c, f_c, a, h, or h_{con} are omitted from the model designation, their default values are assumed to be 6 mm, 37 MPa, 45°, 78 mm, and 100 mm, respectively.

3-2 Failure modes and load-slip behaviour and maximum shear strength

In this subsection, the effect of the geometrical parameters and characteristic concrete strength, f_c, on the load-slip curve and maximum shear strength is examined. Before examining the effect of the parameters, the damage process of the concrete core and stresses in the CSC are evaluated on two failure modes of the concrete core and failure of the CSC.

3-2-1- Damage process in two failure modes of the concrete core and failure of the CSC

To examine the damage process and stresses, one model t_p6-a50-b_c20-t_c4 is evaluated by failure modes of the CSC and one model t_p6-a50-b_c40-t_c4 is evaluated by failure mode of the concrete core. The difference of these models is only in the width of the shear connectors b_c that is 20 and 40 mm

respectively according to their designation. As per Fig. 6a, for load 69 kN, crack develops in the concrete core from the four corners of the shear connectors. However, stresses in the CSC reached the yield limit according to the properties of the steel. As the load increased to the maximum value 80 kN, the CSC stresses are in the failure limit, so that as deformation increased in the CSC, load declined and concrete failed at load 62 kN. Fig. 7(a) shows that, as the width of the shear connector increased to 40 mm, the load-carrying capacity increased, so that cracks began in the concrete core at 85 kN and the yielded surfaces developed in the CSC. As per Fig. 7(b), as the load increased to the maximum value 95 kN, the yielded surfaces increased in the CSC, but before its failure cracks in the concrete core significantly developed. However, according to Fig. 7(c), despite failure of the concrete core, the CSC yielded but did not reach the failure stress.

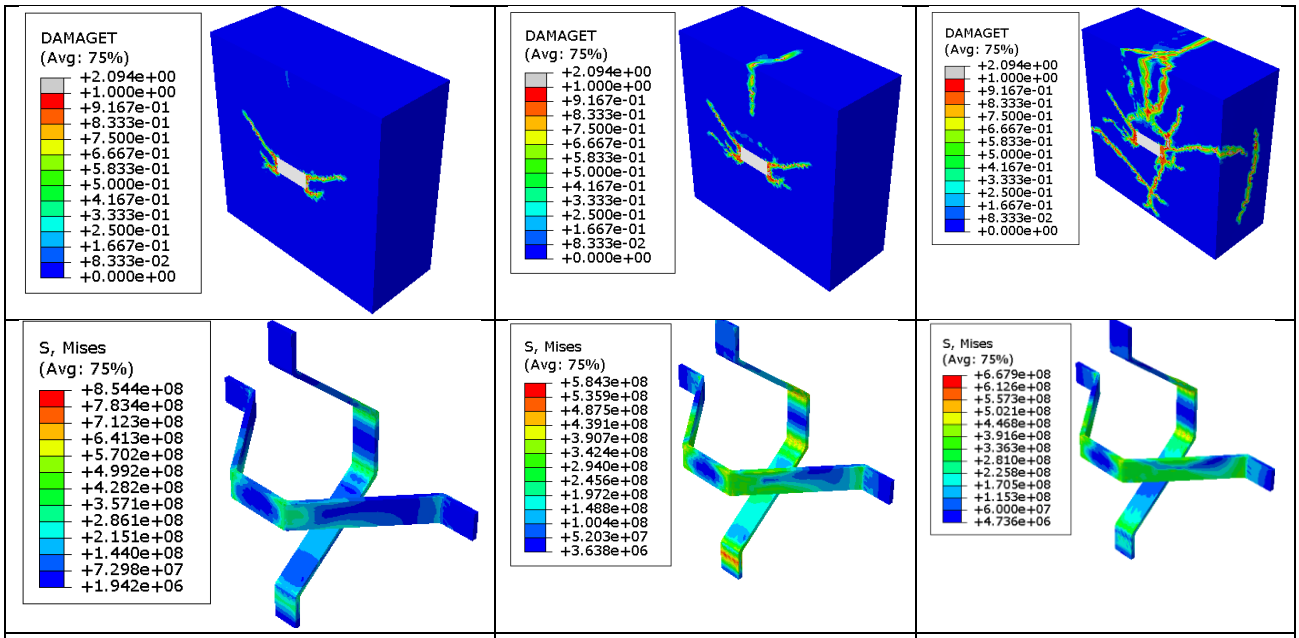

(a) CSC's yielding: 69 kN (b) Maximum load: 80 kN (c) Load decline: 62 kN

Figure 6. Damage progression of the concrete core and stress distribution in the CSCs corresponding to the failure mode observed in model tp6-a50-bc20-tc4.

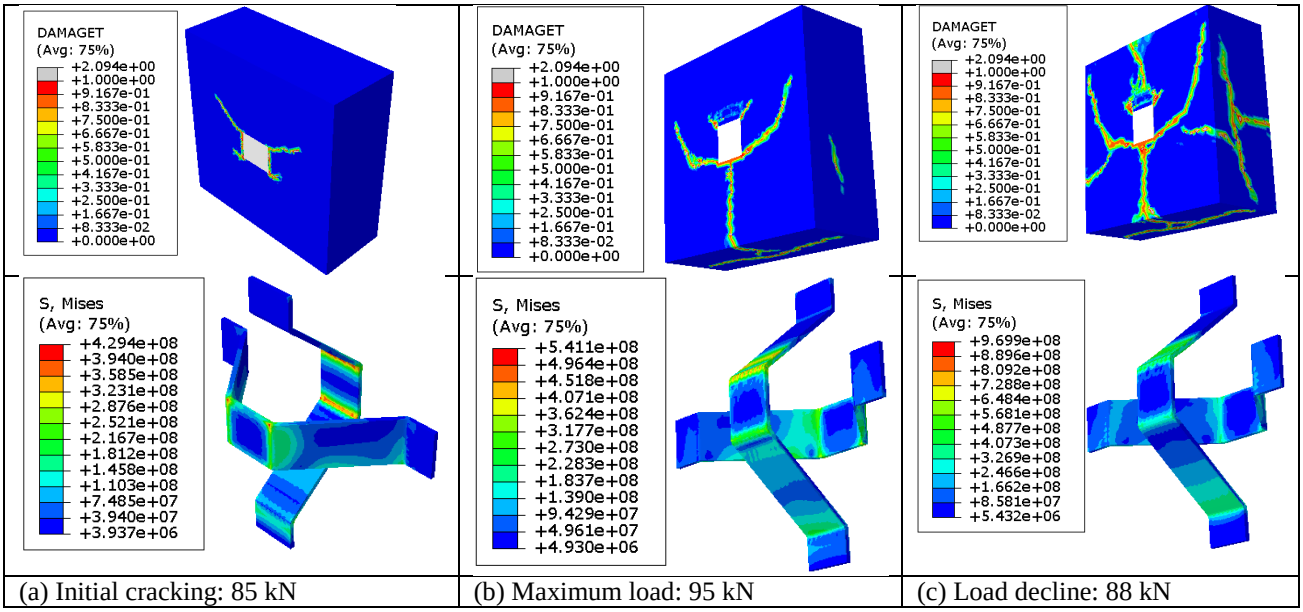

(a) Initial cracking: 85 kN (b) Maximum load: 95 kN (c) Load decline: 88 kN

Figure 7. Damage process of the concrete core and stresses in the CSC for the failure mode of the concrete core in the model t_p6-a50-b_c40-t_c4

Generally, the comparison of Figs. 6 and 7 shows that, as the width of CSC shear connectors increases, crack development decreases in the concrete core and moves toward wedge failure.

3-2-2- Influence of the thickness of the steel face plates

The effect of the thickness of the steel face plates (t_p) on the behaviour of the shear connectors is examined for 4, 6, 8, 10, 12, 14 and 16 mm. In Fig. 8(a) and (b), the effect of different thicknesses of the steel face plates on the load-slip behaviour of the DSCS is compared for the thickness of 4 mm for shear connectors and, in Fig. 8(c) and (d), it is compared for the thickness of 6 mm of the shear connectors. According to Fig. 8, as the thickness of the steel face plates increases from 4 mm to 6 mm, the changes in the load-slip behaviour are very negligible. However, as t_p increased from 6 mm to 8 mm, the ultimate shear strength increased 15% for t_c equal to 4 mm, and 7.5% for t_c equal to 6 mm. As the stiffness of the steel face plates increased, as in Fig. 8(a), the effect of the changes of t_p on the load-slip behaviour and ultimate shear strength become negligible.

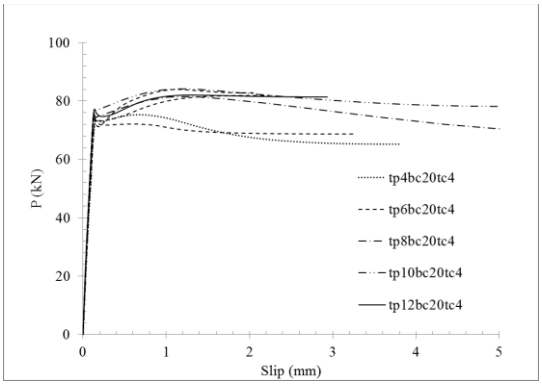

(a) Load-slip curves with $t_c = 4mm$

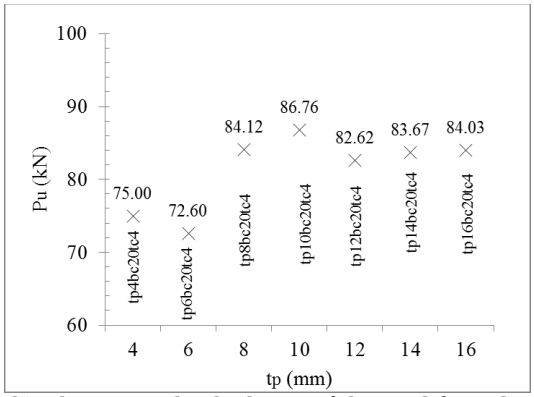

(b) Changes in the thickness of the steel face plates (t_p) with $t_c = 4mm$

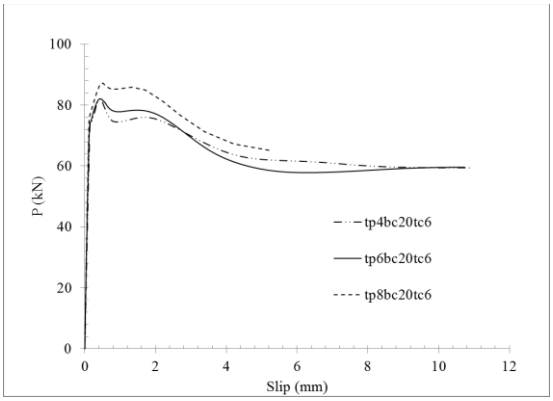

(c) Load-slip curves with $t_c = 6mm$

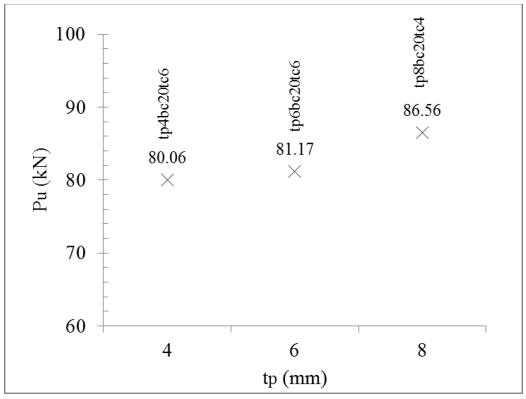

(d) Changes in the thickness of the steel face plates (t_p) with $t_c = 6mm$

Figure 8. Effect of the thickness of the steel face plates (t_p) on the load-slip behaviour and ultimate shear strength of the DSCS models

3-2-3- Influence of the ratio of the width to thickness of shear connectors, b_c / t_c

The effect of changes in the width of shear connectors, b_c, can be examined changing parameters shear connectors' thickness and width of the concrete core, b. Hence, two parameters

$b_t = b_c / t_c$ and $k_{cb} = b_c / b$ are defined. Fig. 9 shows that, as the values of b_t decrease, ductility decreases but ultimate shear strength increases due to the higher thickness of the shear connectors. To prevent brittle and local failure of concrete, b_t values must be so that concrete does not crush before steel yields.

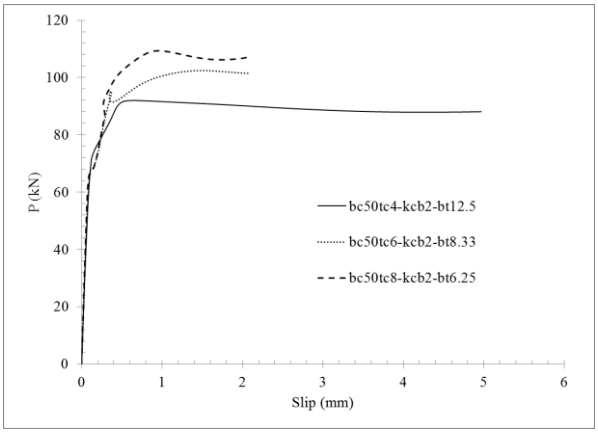

Figure 9. Effect of large values of $b_t = b_c / t_c$ on the load-slip behaviour and ultimate shear strength of the DSCS models

In Fig. 10, the behaviour of the models is shown for larger values of b_t and k_{cb}. In models b_c10t_c6-$k_{cb}0.4$-$b_t1.67$ and b_c10t_c8-$k_{cb}0.4$-$b_t1.25$, b_t values are 1.67 and 1.25, respectively, and k_{cb} is constant at 0.4. Compared to model b_c10t_c4-$k_{cb}0.4$-$b_t2.5$ with b_t equal to 2.5, these models had an increase in ultimate shear strength of about 7% and 15% respectively as in Fig. 10(b). The increase in k_{cb} in model b_c20t_c8-$k_{cb}0.8$-bt2.5 compared to model b_c10t_c4-$k_{cb}0.4$-bt2.5 resulted in an increase of 48% in ultimate shear strength. However, ductility significantly decreased due to an increase in stiffness of the shear connectors, so that the interlayer-slip at the ultimate shear strength reached from 1.64 mm to 0.52 mm. Diagrams show that the increase in the dimensions of the shear connectors with k_{cb} values larger than 2 and b_t larger than 6.25 did not significantly affect increase in the ultimate shear strength due to the increase of stiffness of the shear connectors.

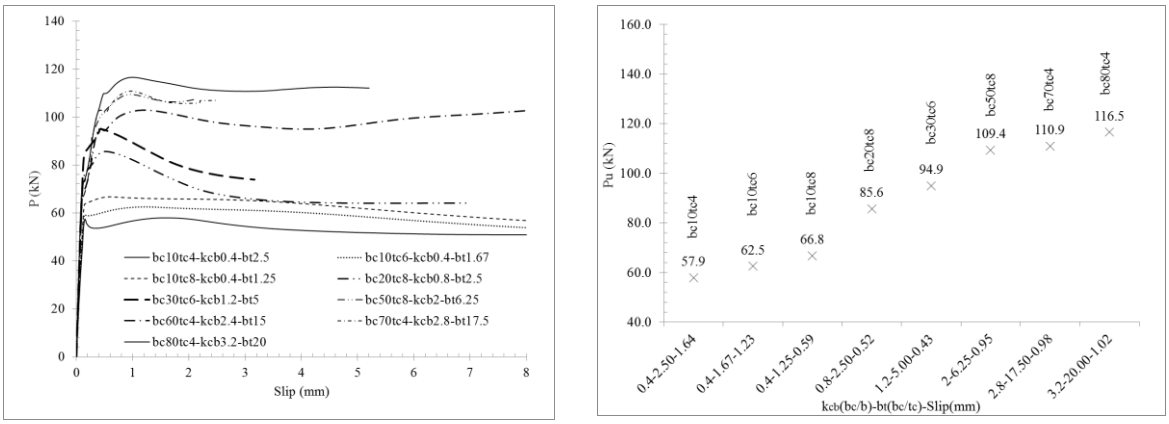

(a) Load-slip curves (b) Ultimate shear strength

Figure 10. Comparison of the effect of $k_{cb} = b_c / b$ and $b_t = b_c / t_c$ on the load-slip behaviour and ultimate shear strength of the DSCS models

3.2.4 Influence of the angle of the branches of the shear connectors, θ

In this subsection, the effect of angles ($50°,60°,70°,90°$) of the branches of the shear connectors on the load-slip behaviour and maximum shear strength is examined. Fig. 11 shows that, as the angles of the shear connectors increase from $50°$ to $60°$ and $70°$, ductility increases and ultimate shear strength increased by 4.5% and 13.5% from 77.5 kN to 81 kN and 88 kN. However, as the angle increased to $90°$, in addition to the significant decrease in ductility, the ultimate shear strength decreased by about 6%.

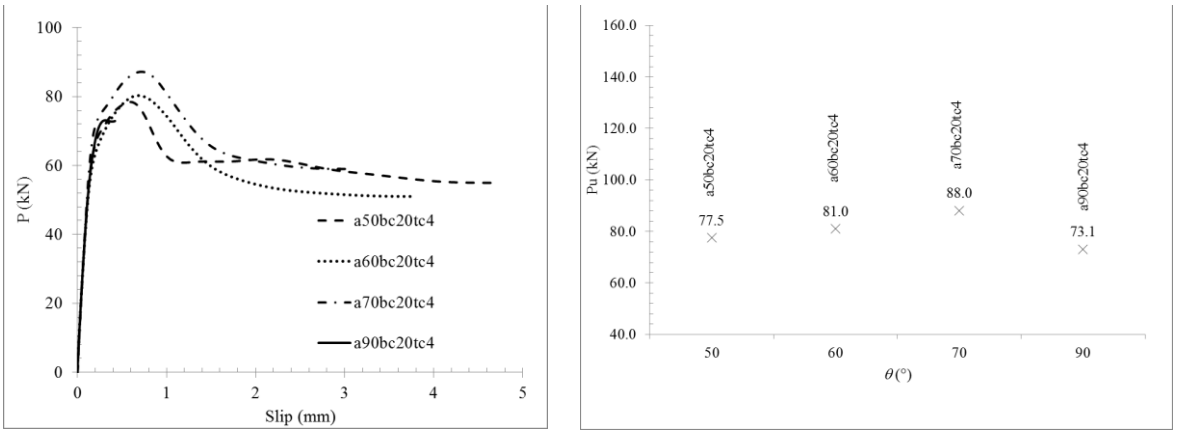

(a) Load-slip curves (b) Ultimate shear strength

Figure 11. Effect of the angle of the branches θ on the load-slip behaviour and ultimate shear strength of the DSCS models

3-2-5- Influence of the ratio of the height of shear connectors, h_c, to the concrete core thickness, h_{con}

According to Fig. 12(a) and (b), as the concrete core thickness increased from 60 mm, with maximum shear strength of 80.3 kN, to 65 mm and 70 mm, the maximum shear strength increased by 8.2% and 16%, i.e. 86.9 kN and 93.3 kN. However, as the core thickness increased from 70 to 75 mm, displacement at failure load increased but ultimate shear strength did not change. According to the diagrams, the increase in core thickness increases ductility. However, the concrete core thickness should not increase so that the shear connectors are weak compared to the concrete core.

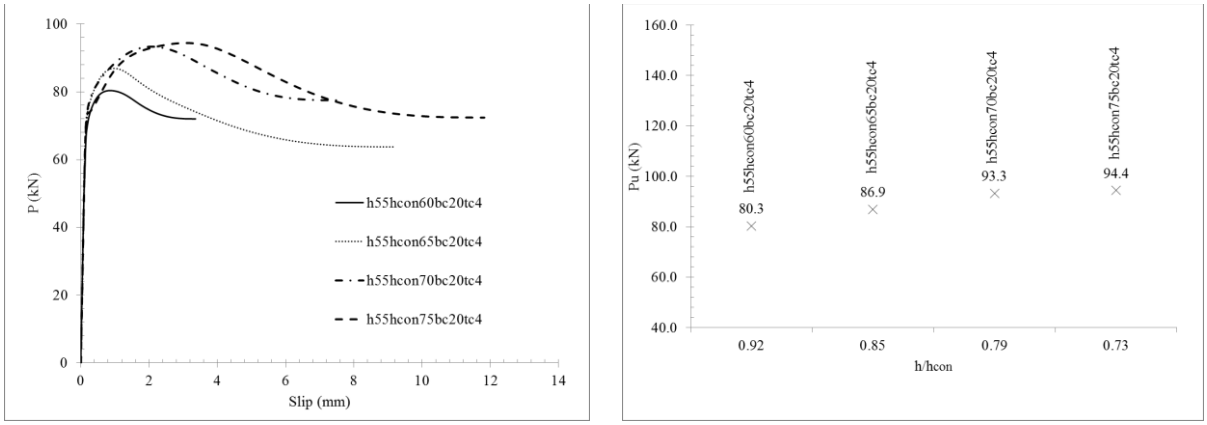

(a) Load-slip curves (b) Ultimate shear strength

Fig. 12. Effect of the concrete core thickness (h_{con}) on the load-slip behaviour and ultimate shear strength of the DSCS models

3-2-6- Influence of the compressive strength of the concrete core, f_c

One of the parameters affecting the load-slip behaviour of the DSCS is the mechanical properties of the concrete core. Here, the compressive strength of the concrete core has changed without changing its geometrical properties. The increasing trend of the curves in Figs. 13(a) and (b) shows that the increase in compressive strength of the concrete core significantly affected the increase in ductility and energy dissipation and the ultimate shear strength; as the compressive strength increased from 25 MPa to 55 MPa, the ultimate shear strength reached from 76.6 kN to 104.3 kN and increased by about 36%. Anyway, the increase in compressive strength of the concrete core should be proportional to the increase in geometrical dimensions and mechanical properties of the shear connectors.

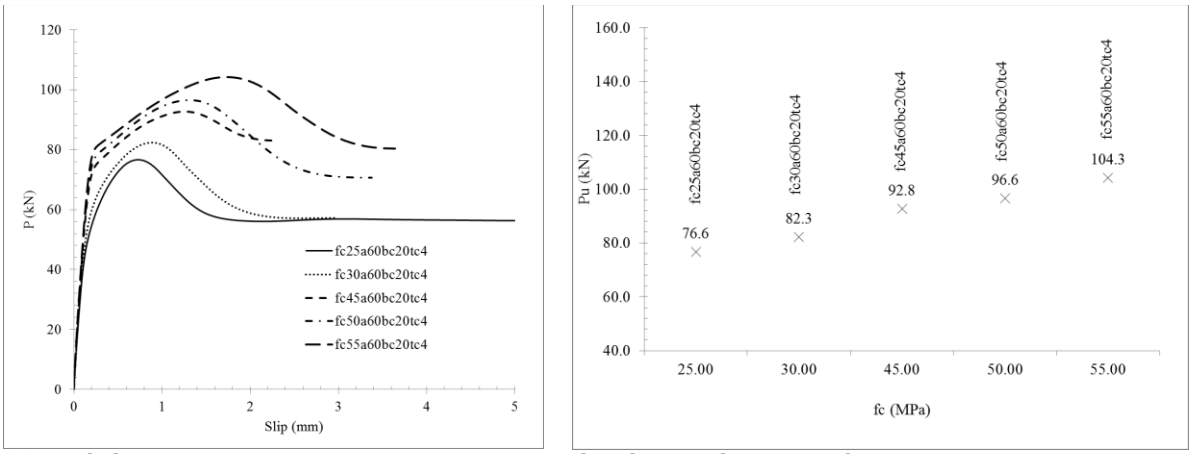

(a) Load-slip curves (b) Ultimate shear strength

Figure 13. Effect of the concrete's compressive strength f_c on the load-slip behaviour and ultimate shear strength of the DSCS models

The examination of the effect of geometrical parameters and compressive strength of the concrete core of the DSCS showed that the effect of all parameters should be considered in a general relation to obtain the ultimate shear strength. Hence, relations are proposed in the next section based on the 211 numerical models with different values of the parameters.

3-3 Proposed relations of the shear strength of the DSCS based on the numerical analysis

For maximum shear strength of the CSC shear connectors under the effect of the push-out test, Yousefi and Ghalehnovi (2017) proposed the following relation by performing a linear regression analysis of 15 test specimens:

$$\frac{P_u}{A_s} = 35.2 t_p^{0.386} l_c^{0.162} hh^{0.312} k_{cb}^{-0.51} \theta_r^{0.287} \quad (1)$$

To this end, regression analysis was conducted on the results of 211 numerical push-out test models to derive empirical relations for estimating the shear strength per unit area of DSCS specimens (P_u / A_s). The parameters influencing the shear strength include: t_p, b_c, t_c, f_c, E_c, θ_r, l_c, h_c, h_{con}, and the derived ratios $b_t = b_c/t_c$, $l_h = l_c/h_{con}$, $h_h = h_c/h_{con}$, and $k_{cb} = b_c/b$. The proposed relations incorporate the most influential variables governing shear strength, while the general form of the equation corresponds to the failure mode associated with concrete crushing as follows:

$$\frac{P_u}{A_s} = A_1 f_c^{A_2} E_c^{A_3} t_p^{A_4} b_c^{A_5} t_c^{A_6} l_c^{A_7} h_c^{A_8} h_{con}^{A_9} b_t^{A_{10}} lh^{A_{11}} hh^{A_{12}} k_{cb}^{A_{13}} \theta_r^{A_{19}} \quad (2)$$

Here, $A_1, ..., A_{19}$ are coefficients determined by regression analysis.

In Eq. (2), logarithmic transformation is used and a linear relation is structured for simplicity of the solution and the linear regression analysis is performed based on the results of 211 finite elements models. Examining different

combinations of the variables, the following five equations are proposed for the failure mode of concrete:

$$\frac{P_{u1}}{A_s} = 0.0425\, f_c^{0.366} h_{con}^{0.7} b_t^{0.847} l_{ch}^{-6.81} hh^{18.04} k_{cb}^{-1.55} \theta_r^{-0.015} \quad (3)$$

$$\frac{P_{u2}}{A_s} = 0.953\, f_c^{0.365} b_t^{0.841} l_{ch}^{-3.27} hh^{9.27} k_{cb}^{-1.55} \theta_r^{-0.0175} \quad (4)$$

$$\frac{P_{u3}}{A_s} = 0.841\, f_c^{0.36} b_t^{0.87} hh^{1.54} k_{cb}^{-1.59} \theta_r^{-0.02} \quad (5)$$

$$\frac{P_{u4}}{A_s} = 0.464\, f_c^{0.35} b_t^{0.92} k_{cb}^{-1.68} \theta_r^{-0.023} \quad (6)$$

$$\frac{P_{u5}}{A_s} = 16.56\, f_c^{0.316} k_{cb}^{-0.79} \theta_r^{-0.3} \quad (7)$$

Since the steel face plates with the minimum thickness (6 mm) did not affect the shear behaviour of the shear connectors and, on the other hand, the face plates should have enough stiffness to examine the shear behaviour of the shear connectors, the variable t_p is not considered in the relations. In addition, the modulus of elasticity of concrete E_c is directly related to f_c experimentally and was not effective in the relations. In the following subsection, the proposed relations are described.

3-4 Comparison of the proposed models of the maximum shear strength with the numerical analysis results

In this section, the results of the proposed relations to predict the shear strength of DSCS are compared with the numerical analysis results. In Fig. 14, the dispersion of the results from five proposed Eqs. (3) to (7) and dispersion of the results of Eq. (2) are compared with the results of 211 numerical models in the error range $\pm 10\%$. In addition, due to the large volume, only part of the data of the comparison of the results of the numerical analysis of 211 numerical models and prediction based on the relations are given in Table 2. In table 2, FM is the failure mode, P_{FE} is the numerical shear strength of DSCS, P_{prop} is the prediction by Eq. 6 (Yousefi & Ghalehnovi, 2017), P_{u1} is prediction by proposed Eq. (3), P_{u2} is the prediction by proposed Eq. (4), P_{u3} is the prediction by proposed Eq. (5), P_{u4} is the prediction by Eq. (6), P_{u5} is the prediction by Eq. (7), CC is the failure mode of concrete cracking, SC is the failure mode of the shear connector. Dispersion of the data shows that the highest dispersion is related to Eq. (7) obtained based on a limited number of tests. The mean value and variance of the ratio of the numerical analysis to the prediction are 0.83 and 0.08, based on the Eq. (7) as in Table 2. According to Figs. 14(a) and (b), the highest concentration of data in the error range $\pm 10\%$ is related to Eq. (3) with variables f_c, h_{con}, b_t, l_{ch}, h_h, k_{cb} and θ_r and Eq. (4) with variables f_c, b_t, l_{ch}, h_h, k_{cb} and θ_r. According to Table 2, the mean value and variance of the sum of the ratios of the numerical analysis to the prediction are 1.03 and 0.01, based on Eq. (3), and are 1.03 and 0.02, based on Eq. (4). The similar accuracy of the relations shows that, despite variable *hh* being the ratio of h_c to h_{con}, variable h_{con} can be deleted in the regression analysis. The mean value and variance of the sum of the ratios of numerical analysis to the prediction are 1.03 and 0.02, based on Eq. (5), and are 1.04 and 0.02 based on Eq. (6), which are slightly higher than for Eqs. (3) and (4). However, Eqs. (5) and (6) have less variables and give simpler relations, so that variables h_{con} and I_{ch} are deleted in relation (5) and the h_{con}, I_{ch} and $\boldsymbol{h_h}$ are deleted in Eq. (6). However, in Eq. (7), by deleting variable b_t in addition to the three variables h_{con}, I_{ch} and $\boldsymbol{h_h}$, dispersion has sharply increased according to Figs. 14(e) and (f). According to Table 2, the mean value and variance of the ratios of the numerical analysis to the prediction are 1.08 and 0.11, respectively.

Conclusions

This study conducted a numerical investigation into the shear performance of corrugated strip connectors (CSC) embedded in steel-concrete-steel (SCS) sandwich composite structures. These systems are increasingly adopted in offshore engineering due to their high strength-to-weight ratio and exceptional energy dissipation capacity. A total of 211 finite element models were developed in ABAQUS using the Explicit solver combined with a mass-scaling technique to

efficiently simulate quasi-static behavior despite geometric complexities. The parametric analysis examined the influence of key design variables—including steel face plate thickness, concrete core thickness, and concrete compressive strength—on the shear capacity of the connectors. A summary of the main findings is presented below.

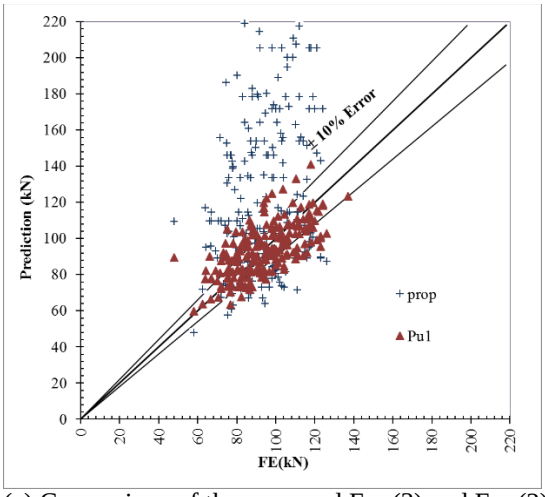

(a) Comparison of the proposed Eq. (3) and Eq. (2)

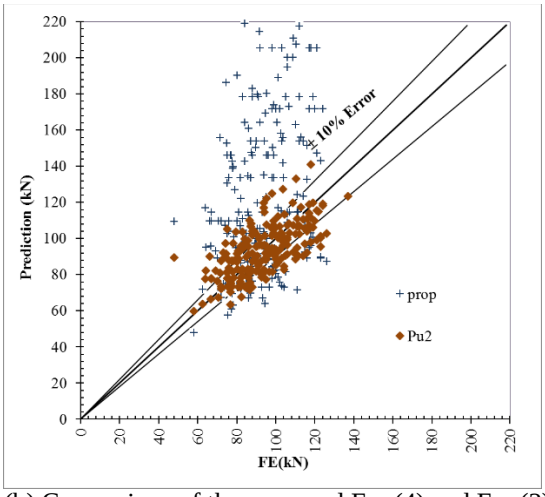

(b) Comparison of the proposed Eq. (4) and Eq. (2)

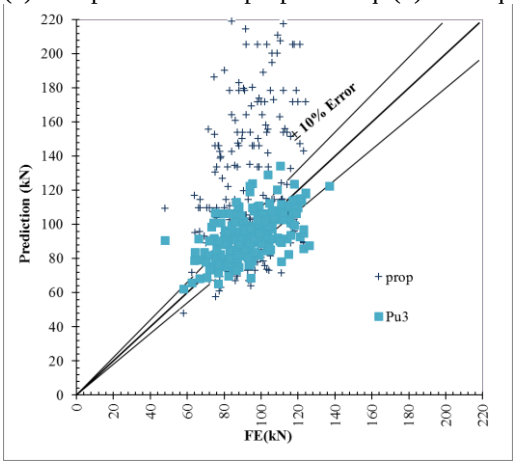

(c) Comparison of the proposed Eq. (5) and Eq. (2)

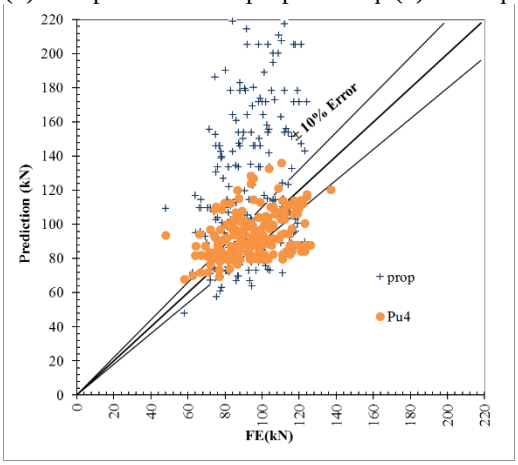

(d) Comparison of the proposed Eq. (6) and Eq. (2)

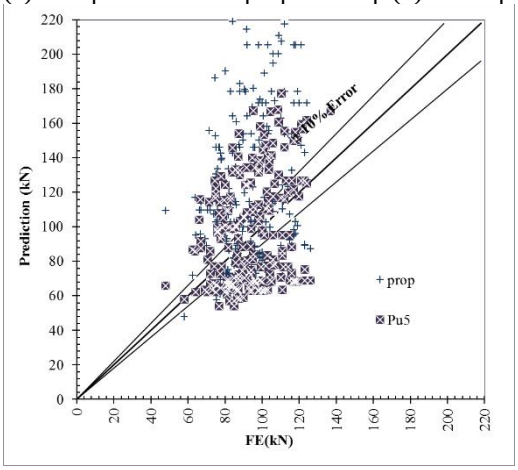

(e) Comparison of the proposed Eq. (7) and Eq. (2)

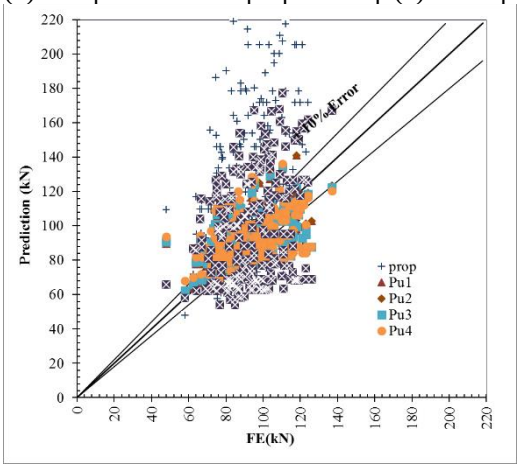

(f) Comparison of the dispersion of all proposed equations

Figure 14. Comparison of the dispersion of the results of shear strength of DSCS from the proposed equations and numerical analysis

Table 2. Comparison of the results of the numerical analysis of DSCS and predictions using the proposed equations

No.	Test ref.	FM	P_{FE}	P_{prop}	$\frac{P_{FE}}{P_{prop}}$	P_{u1}	$\frac{P_{FE}}{P_{u1}}$	P_{u2}	$\frac{P_{FE}}{P_{u2}}$	P_{u3}	$\frac{P_{FE}}{P_{u3}}$	P_{u4}	$\frac{P_{FE}}{P_{u4}}$	P_{u5}	$\frac{P_{FE}}{P_{u5}}$
1	t_p4-b_c20-t_c4	SC	75	58	1.31	74	1.02	74	1.02	76	1.00	80	0.94	67	1.13
2	t_p6-b_c20-t_c4	SC	72	67	1.07	74	0.98	74	0.98	76	0.95	80	0.90	67	1.08
3	t_p4-b_c20-t_c6	CC	82	86	0.95	78	1.05	78	1.05	80	1.03	83	0.99	100	0.82
4	t_p6-b_c20-t_c6	CC	78	101	0.78	78	1.00	78	1.00	80	0.98	83	0.94	100	0.78
5	t_p6-b_c20-t_c8	CC	86	135	0.64	82	1.05	82	1.04	83	1.03	85	1.01	133	0.64
210	t6-b_c40-t_c8-b280	CC	109	200	0.54	120	0.91	120	0.91	120	0.90	121	0.90	168	0.65
211	t6-b_c40-t_c8-b300	CC	110	208	0.53	133	0.83	133	0.83	134	0.82	136	0.81	177	0.62
Mean					**0.83**		**1.03**		**1.03**		**1.03**		**1.04**		**1.08**
Cov					**0.08**		**0.01**		**0.02**		**0.02**		**0.02**		**0.11**

- Angles $60°$ and $75°$ of the branches of the shear connectors to the steel face plates showed a better shear behaviour than angles $45°$ and $90°$. This can be due to the increase in the wedge crack development in the connectors with angle $45°$ and the decrease in inertia moment of the metal section in the shear connectors with angle $90°$;
- An increase of compressive strength of the concrete core increased the ultimate shear strength and ductility due to a higher bending capacity of the shear connectors and an increase in bond;
- The comparison of the proposed equations based on 211 numerical models with the proposed equation based on 15 test specimens showed that in the proposed equations the error of the prediction of the interlayer ultimate shear strength significantly decreased as the parameter concrete compressive strength, f_c, was considered.

Future research could focus on experimental validation of the numerical models, assessment of fatigue and long-term durability under cyclic and environmental loading, and optimization of connector geometry for enhanced performance. Investigating dynamic behavior under impact or seismic conditions, exploring advanced interface modeling techniques, and integrating high-performance materials such as UHPC or fiber-reinforced concrete would further improve design reliability. Additionally, data-driven approaches and machine learning could support predictive modeling and design automation for SCS systems in offshore and seismic applications.

Acknowledgments:

The authors would like to express their sincere gratitude to Chabahar Maritime University (CMU) and Ferdowsi University of Mashhad for their valuable support and contributions to this research.

Funding sources

This research did not receive any specific grant from funding agencies in the public, commercial, or not-for-profit sectors.

Declaration of Competing Interest

This expression states that there is no conflict of interest to disclose regarding the submission of our paper to your esteemed journal. All authors have no financial or personal relationships that could potentially bias the content or findings of this research.

Authors contribution statement

Mohammad Golmohammadi carried out numerical analysis in this study. All authors discussed the results and contributed to the final manuscript. Mehdi Yousefi conceived of the presented idea and developed the theory and performed the computations. Also, Mehdi Yousefi verified the analytical methods. .

References

ABAQUS, S. (2010). EUs Manual. *Hibbitt, Karlsson & Sorensen Inc, Pawtucket, RI, USA*.

Barahouei, M., Yousefi, M., & Khatibi, S. H. (2025). Experimental and numerical study of the flexural behavior of SCS beams with two-end welding C-shape connectors and reactive powder concrete core. *Case Studies in Construction Materials*, *22*, e04518.

Bowerman, H., & Chapman, J. (2000). Bi-steel concrete steel sandwich construction. The fourth US Engineering Foundation conference on composite construction, June,

Daliri, M., Arab, H. G., Miri, M., & Khatibi, S. H. (2025). Overlap effects of one-end welded box-profile shear connectors on interlayer shear behavior. *Structures*, *71*. https://doi.org/doi.org/10.1016/j.istruc.2024.107982

Daliri, M., Ghohani Arab, H., Miri, M., & Khatibi, S. H. (2025). Prediction of Shear Strength in SCS Panels with One-End Welded BP Shear Connector Using Numerical Modeling and Gene Expression Programming (GEP). *AUT Journal of Civil Engineering*. https://doi.org/10.22060/ajce.2025.23851.5904

Dogan, O., & Roberts, T. (2012). Fatigue performance and stiffness variation of stud connectors in steel–concrete–steel sandwich systems. *Journal of Constructional Steel Research*, *70*, 86-92. https://doi.org/https://doi.org/10.1016/j.jcsr.2011.08.013

Foundoukos, N., & Chapman, J. (2008). Finite element analysis of steel–concrete–steel sandwich beams. *Journal of Constructional Steel Research*, *64*(9), 947-961. https://doi.org/https://doi.org/10.1016/j.jcsr.2007.10.011

Huang, Z., & Liew, J. (2016). Numerical studies of steel-concrete-steel sandwich walls with J-hook connectors subjected to axial loads. *Steel and Composite Structures*, *21*(3), 461-477.

Huang, Z., Liew, J. R., Yan, J., & Wang, J. (2013). Finite element analysis of curved lightweight steel–concrete–steel sandwich panel subjected to lateral loads. *Proceeding of Advances in Structural Engineering and Mechanics (ASEM13), Steel and Composite Structures (ICSCS13)*, 2583-2597.

Khatibi, S. H., Arab, H. G., & Miri, M. (2022). Interlayer behavior investigation of box profile shear connectors in steel-concrete-steel sandwich structures. *Structures*, *45*, 1031-1042. https://doi.org/https://doi.org/10.1016/j.istruc.2022.09.064

Khatibi, S. H., Arab, H. G., & Miri, M. (2023). The behavior of steel-concrete-steel sandwich composite beams with box-profile shear connectors: Experimental and numerical. *Structures*, *54*, 644-656. https://doi.org/https://doi.org/10.1016/j.istruc.2023.05.054

Leekitwattana, M., Boyd, S., & Shenoi, R. (2011). Evaluation of the transverse shear stiffness of a steel bi-directional corrugated-strip-core sandwich beam. *Journal of Constructional Steel Research*, *67*(2), 248-254.

Liew, J. R. (2008). Innovative SCS system for marine and offshore applications. *The Structural Engineer*, *86*(12), 24-25.

Liew, J. R., & Sohel, K. (2009). Lightweight steel–concrete–steel sandwich system with J-hook connectors. *Engineering Structures*, *31*(5), 1166-1178.

Roshani, H., Yousefi, M., Gharaei-Moghaddam, N., & Khatibi, S. H. (2023). Flexural performance of steel-concrete-steel sandwich beams with lightweight fiber-reinforced concrete and corrugated-strip connectors: Experimental tests and numerical modeling. *Case Studies in Construction Materials*, *18*, e02138.

Shanmugam, N., Kumar, G., & Thevendran, V. (2002). Finite element modelling of double skin composite slabs. *Finite elements in analysis and design*, *38*(7), 579-599.

Smitha, M., & Kumar, S. S. (2013). Steel–concrete composite flange plate connections—finite element modeling and parametric studies. *Journal of Constructional Steel Research*, *82*, 164-176.

Solomon, S., Smith, D., & Cusens, A. (1976). Flexural tests of steel-concrete-steel

sandwiches. *Magazine of Concrete Research*, *28*(94), 13-20.

Tomlinson, M., Tomlinson, A., Li Chapman, M., Jefferson, A., & Wright, H. (1990). Shell composite construction for shallow draft immersed tube tunnels. In *Immersed tunnel techniques* (pp. 209-220). Thomas Telford Publishing.

Yan, J.-B. (2015). Finite element analysis on steel–concrete–steel sandwich beams. *Materials and Structures*, *48*(6), 1645-1667.

Yan, J.-B., Liew, J., & Zhang, M.-H. (2015a). Ultimate strength behavior of steel-concrete-steel sandwich beams with ultra-lightweight cement composite, Part 2: finite element analysis. *Steel and Composite Structures*, *18*(4), 1001-1021.

Yan, J.-b., Liew, J. R., Sohel, K., & Zhang, M. (2014). Push-out tests on J-hook connectors in steel–concrete–steel sandwich structure. *Materials and Structures*, *47*(10), 1693-1714.

Yan, J.-B., Liew, J. R., & Zhang, M.-H. (2015b). Shear-tension interaction strength of J-hook connectors in steel-concrete-steel sandwich structure. *Advanced Steel Construction*, *115*(1), 73.

Yan, J.-B., Liew, J. R., Zhang, M.-H., & Wang, J. (2014). Ultimate strength behavior of steel-concrete-steel sandwich beams with ultra-lightweight cement composite, Part 1: Experimental and analytical Study. *Steel and Compsite Structures*, *17*(6), 907-927.

Yan, J.-B., Xiong, M.-X., Qian, X., & Liew, J. (2016). Numerical and parametric study of curved steel-concrete-steel sandwich composite beams under concentrated loading. *Materials and Structures*, *49*(10), 3981-4001.

Yousefi, M., & Ghalehnovi, M. (2017). Push-out test on the one end welded corrugated-strip connectors in steel-concrete-steel sandwich structure. *Steel and Composite Structures*, *24*.

Yousefi, M., & Ghalehnovi, M. (2018). Finite element model for interlayer behavior of double skin steel-concrete-steel sandwich structure with corrugated-strip shear connectors. *Steel Compos. Struct*, *27*(1), 123-133.

Yousefi, M., Golmohammadi, M., Khatibi, S. H., & Yaghoobi, M. (2023). Prediction of the punching load strength of SCS slabs with stud-bolt shear connectors using numerical modeling and GEP algorithm. *Journal of Rehabilitation in Civil Engineering*, *11*(3), 68-87.

Yousefi, M., & Khatibi, S. H. (2021). Experimental and numerical study of the flexural behavior of steel–concrete-steel sandwich beams with corrugated-strip shear connectors. *Engineering Structures*, *242*, 112559.

Zou, G. P., Xia, P. X., Shen, X. H., & Wang, P. (2016). Investigation on the failure mechanism of steel-concrete steel composite beam. *Steel and Composite Structures*, *20*(6), 1183-1191.